

Detectors in Nuclear and Particle Physics

Prof. Dr. Johanna Stachel

Department of Physics und Astronomy
University of Heidelberg

July 11, 2018

9. Hadronic Calorimeters

1 Hadronic Calorimeters

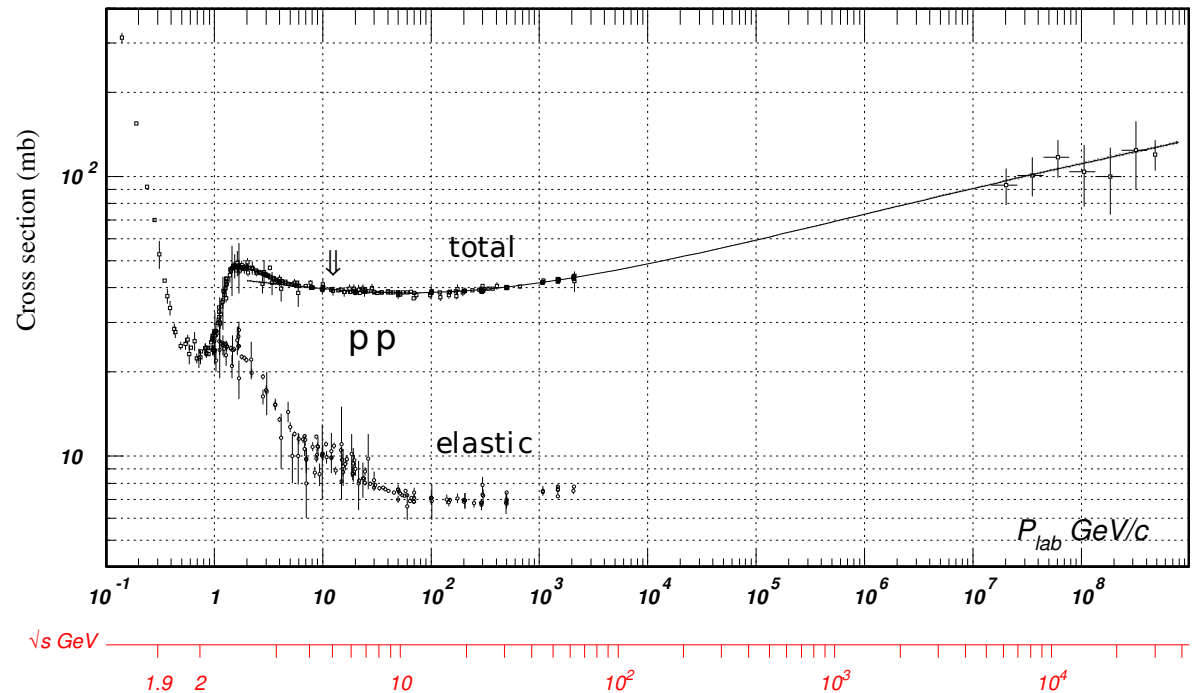
- Hadronic showers
- Hadronic Calorimeters
- Compensation
- Particle identification
- Role of (hadronic) calorimeters in large experiments

9.1 Hadronic showers

Interaction of a hadron with nucleon or nucleus ($E \gtrsim 1$ GeV)

$$\left. \begin{array}{l} \text{elastic} \quad p + N \rightarrow p + N \\ \text{inelastic} \quad p + N \rightarrow X \end{array} \right\} \begin{array}{l} \sigma_{el} \\ \sigma_{inel} \end{array} \quad \sigma_{tot} = \sigma_{el} + \sigma_{inel} \quad \text{grows weakly with } \sqrt{s}$$

\sqrt{s} (GeV)	σ_{tot} for pp (mb)
5	40
100	50
10000	100



- elastic part about 10 mb
- at high energies also diffractive contribution (comparable to elastic)
- but majority of σ_{tot} is due to σ_{inel}
- pA: $\sigma_{tot}(pA) \simeq \sigma_{tot}(pp) \cdot A^{\frac{2}{3}}$

Hadronic interaction length:

$$\lambda_w = \frac{A}{N_A \rho \sigma_{tot}}$$

λ_w is the 'collision length' characterized by σ_{tot} for inelastic processes \rightarrow

$$\lambda_A = \frac{A}{N_A \rho \sigma_{inel}} \quad \text{'hadronic interaction length'}$$

$$N(x) = N_0 \exp\left(-\frac{x}{\lambda_A}\right)$$

$$\lambda_A \simeq 35 \cdot A^{\frac{1}{3}} (\text{gcm}^{-2}) \quad \text{for } Z \geq 15 \text{ and } \sqrt{s} \simeq 1 - 100 \text{ GeV}$$

	C	Ar (lq)	Fe	U	scint.
λ_A (cm)	38.8	85.7	16.8	11.0	79.5
X_0 (cm)	19.3	14.0	1.76	0.32	42.4

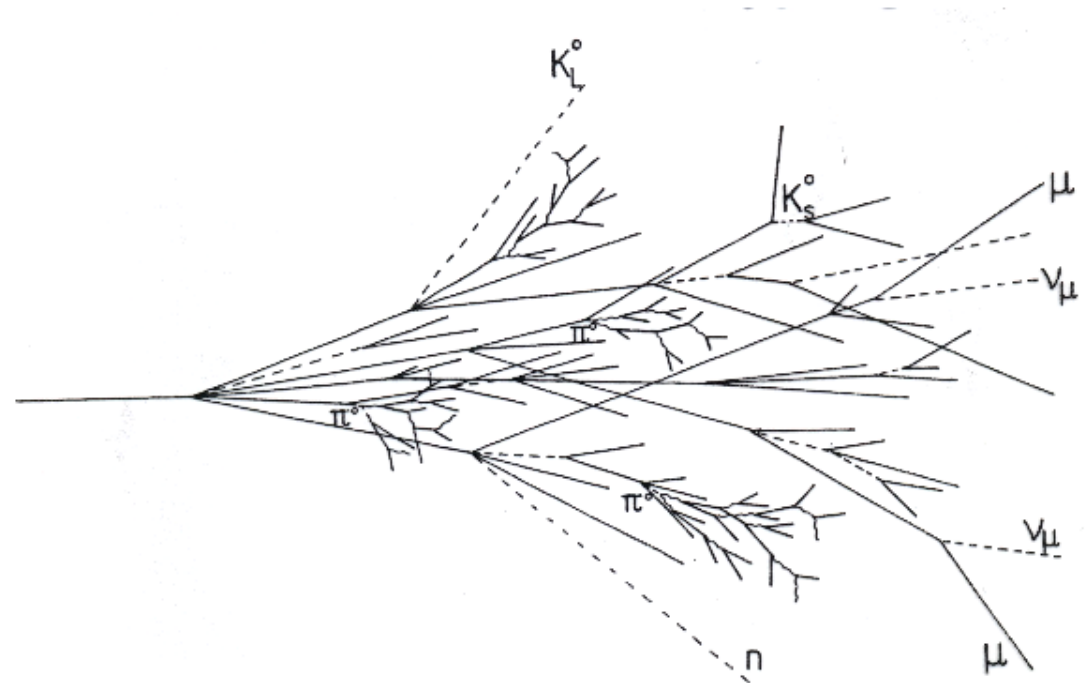
$$\lambda_A \gg X_0$$

\rightarrow hadronic calorimeter needs more depth than electromagnetic calorimeter

will see below: typical longitudinal size for 95 % containment $9 \lambda_A$
 typical transverse size " $1 \lambda_A$

Hadronic shower

- $p + \text{nucleus} \rightarrow \pi^+ + \pi^- + \pi^0 \dots + \text{nucleus}^*$
 - ↳ nucleus 1 + n,p, α
 - ↳ nucleus 2 + 5p,n ...
 - ↳ fission
- secondary particles undergo further inelastic collisions with similar cross sections until they fall below pion production threshold
- sequential decays
 - $\pi^0 \rightarrow \gamma\gamma \rightarrow$ electromagnetic shower
 - fission fragments $\rightarrow \beta$ -decay, γ -decay
 - nuclear spallation: individual nucleons knocked out of nucleus, de-excitation
 - neutron capture \rightarrow nucleus* \rightarrow fission (U)
- mean number of secondary particles $\propto \ln E$
 typical transverse momentum
 $\langle p_t \rangle \simeq 350 \text{ MeV}/c$
- mean inelasticity (fraction of E in secondary particles) $\simeq 50\%$



Shower development

rough estimates (data see below), qualitatively similar to em. shower, fluctuations are huge
 variables: $t = x/\lambda_A$ depth in units of interaction length, $E_{thr} = 290 \text{ MeV}$

$$E(t) = \frac{E}{\langle n \rangle^t}$$

$$E(t_{max}) = E_{thr} \rightarrow E_{thr} = \frac{E}{\langle n \rangle^{t_{max}}}$$

$$\langle n \rangle^{t_{max}} = \frac{E}{E_{thr}} \quad \text{or} \quad t_{max} = \frac{\ln E/E_{thr}}{\ln \langle n \rangle}$$

number of particles in hadronic shower typically lower by a factor E_{thr}/E_C as compared to electromagnetic shower \rightarrow intrinsic resolution worse by factor $\sqrt{E_{thr}/E_C}$

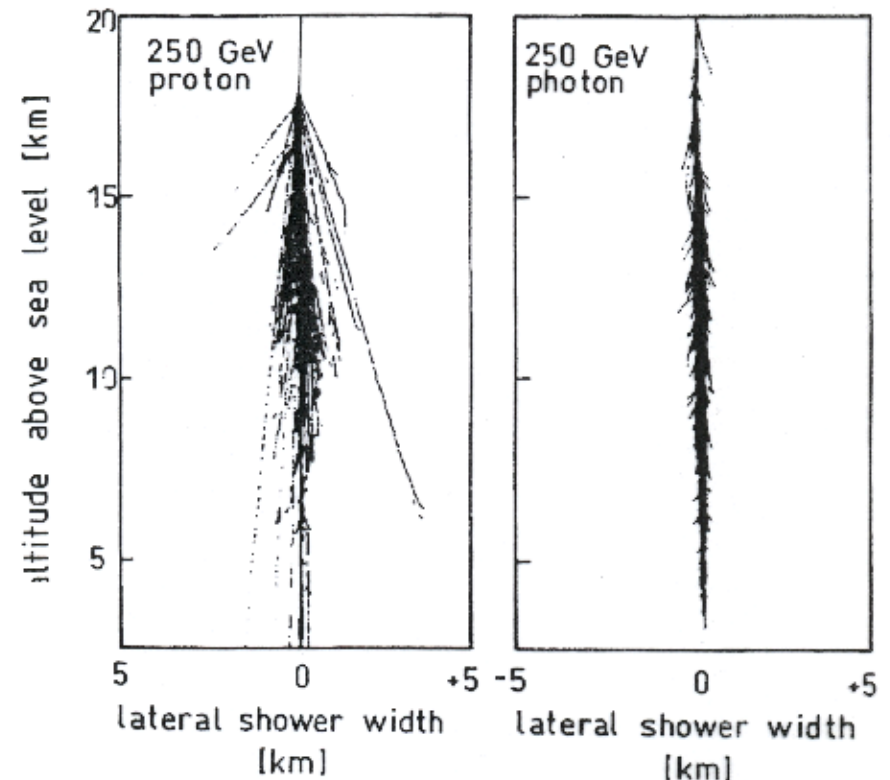
distribution of energy

example: 5 GeV proton in lead-scintillator calorimeter	(MeV)	
ionization energy of charged particles (p, π, μ)	1980	40%
electromagnetic fraction (e, π^0, η^0)	760	15%
neutrons	520	10%
photons from nuclear de-excitation	310	6%
non-detectable energy (nuclear binding, ν, \dots)	1430	29%

Characteristics of hadronic shower

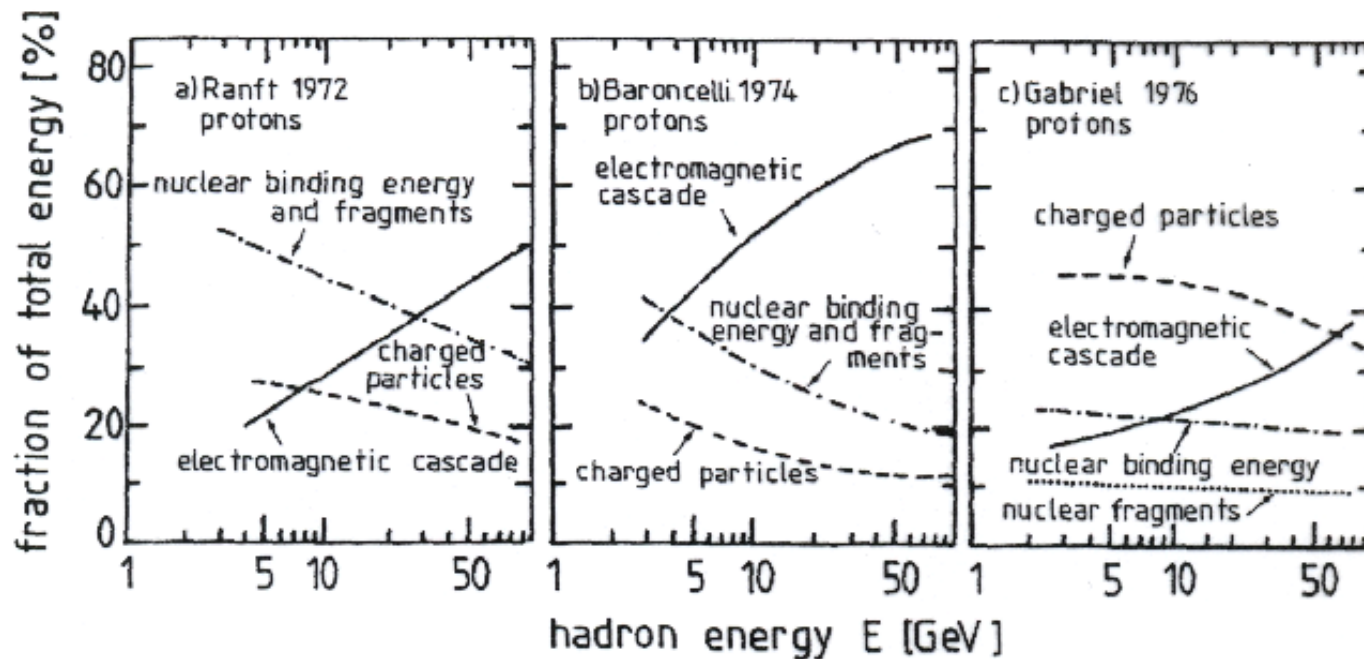
- strong fluctuations in energy sharing
- part of energy invisible, can be partly compensated by neutron capture leading to fission → release of binding energy
- variation in spatial distribution of energy deposition ($\pi^\pm \leftrightarrow \pi^0$ etc.)
- electromagnetic fraction grows with E
 $f_{em} \simeq f_{\pi^0} \propto \ln E$
- energetic hadrons contribute to electromagnetic fraction by e.g. $\pi^- + p \rightarrow \pi^0 + n$, but very rarely the opposite happens (a 1 GeV π^0 travels $0.2 \mu\text{m}$ before decay)
- below pion production threshold, mainly dE/dx by ionization

measurement of hadron energy by calorimetry considerably more difficult as compared to em. case



Monte-Carlo simulated air showers

shower simulations via intra- and inter-nuclear cascade models (GEISHA, CALOR, ...)

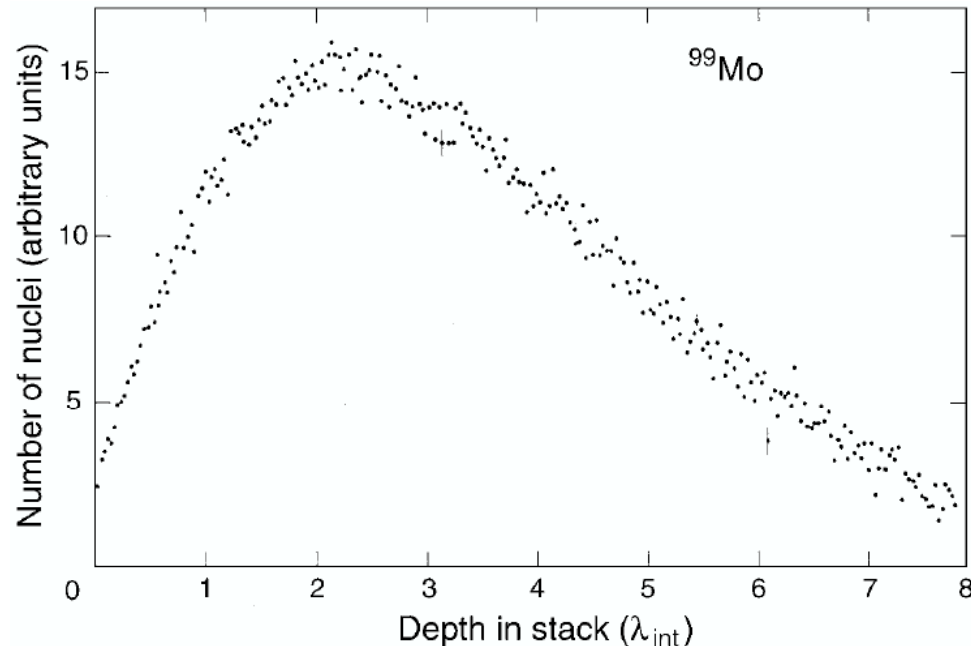


common features, but variations are significant! Need to tune to measured data in any case

Longitudinal shower development

- strong peak near hadronic interaction length λ_A
- followed by exponential decrease
- shower depth: $t_{max} \simeq 0.2 \ln E(\text{GeV}) + 0.7$
 95% of energy over depth $L_{95} = t_{max} + 2.5\lambda_{att}$
 $\lambda_{att} \simeq E^{0.3}$ (E in GeV, λ_{att} in units of λ_A)

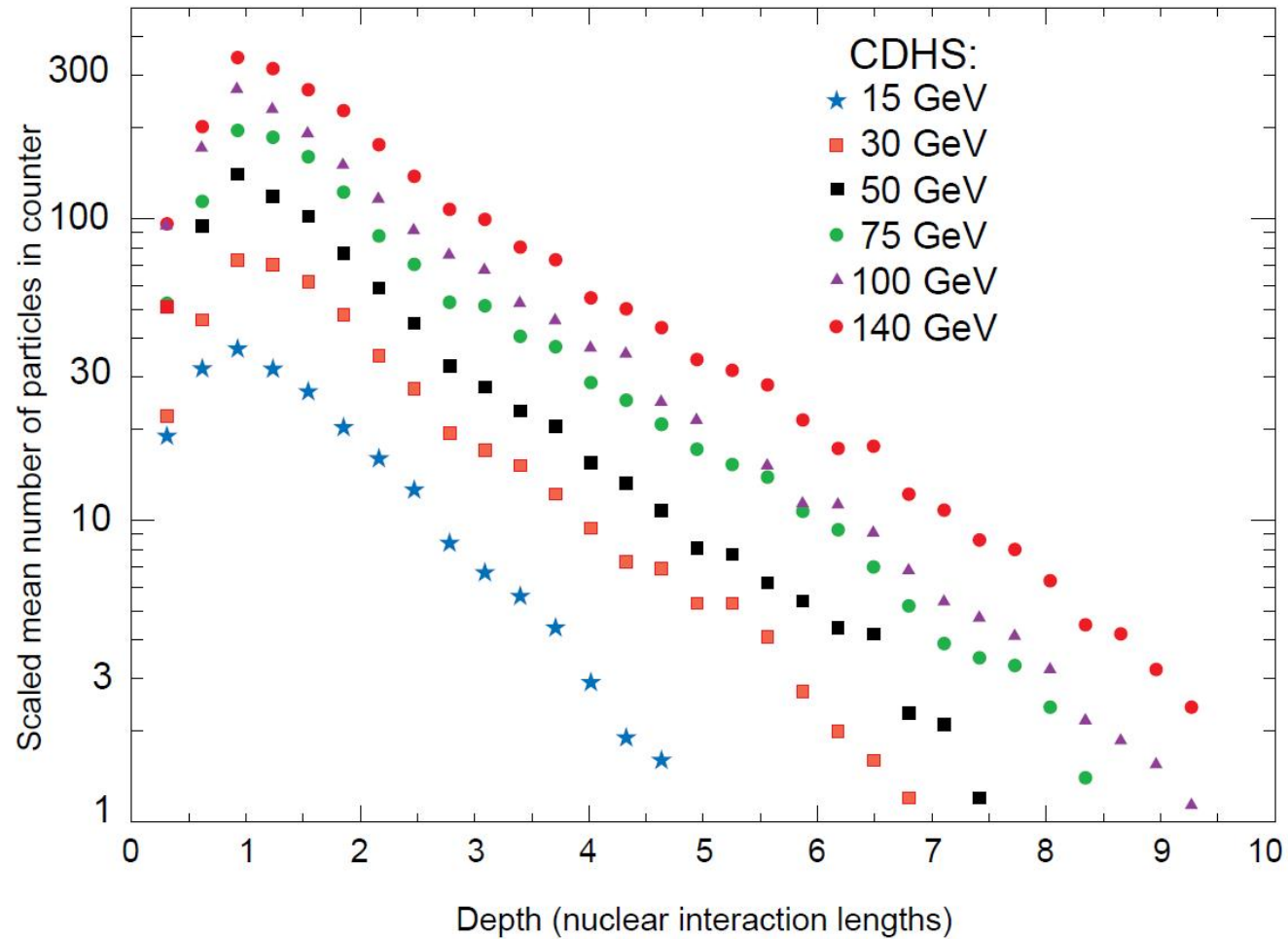
example: 350 GeV π^\pm : $t_{max} = 1.9$ $L_{95} = 1.9 + 5.8$
 need about $8 \lambda_A$ to contain 95 % of energy
 need about $11 \lambda_A$ to contain 99 % of energy



long. shower profile for 300 GeV π^- into block of U; measure radioactivity due to fission fragments

Longitudinal shower development

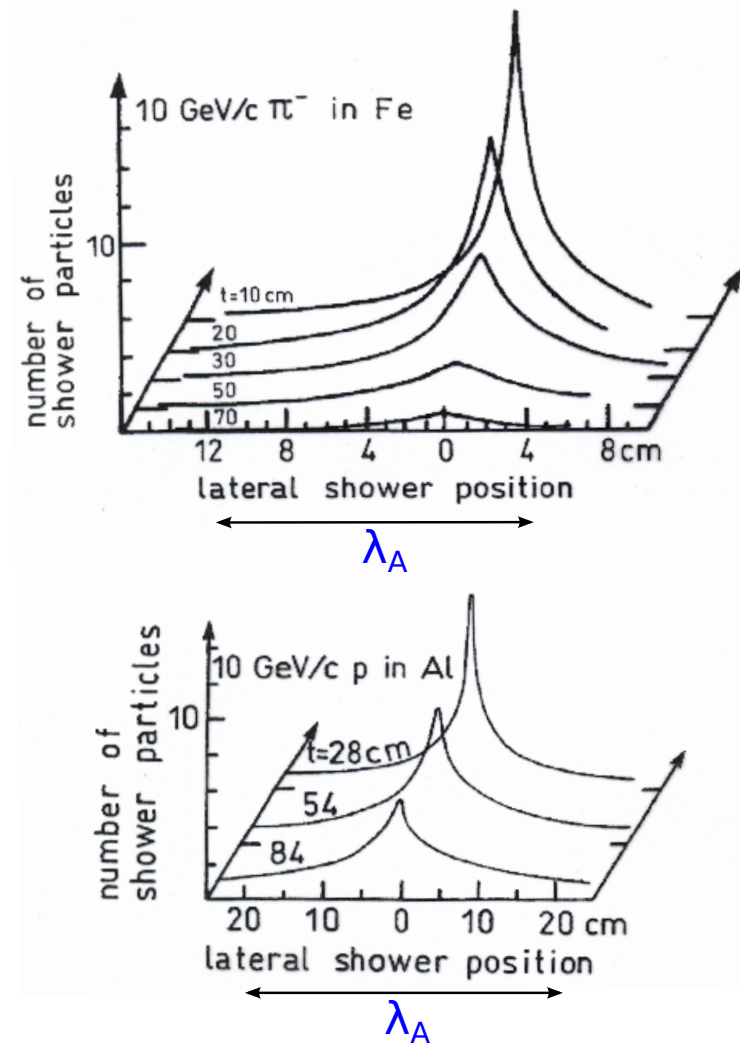
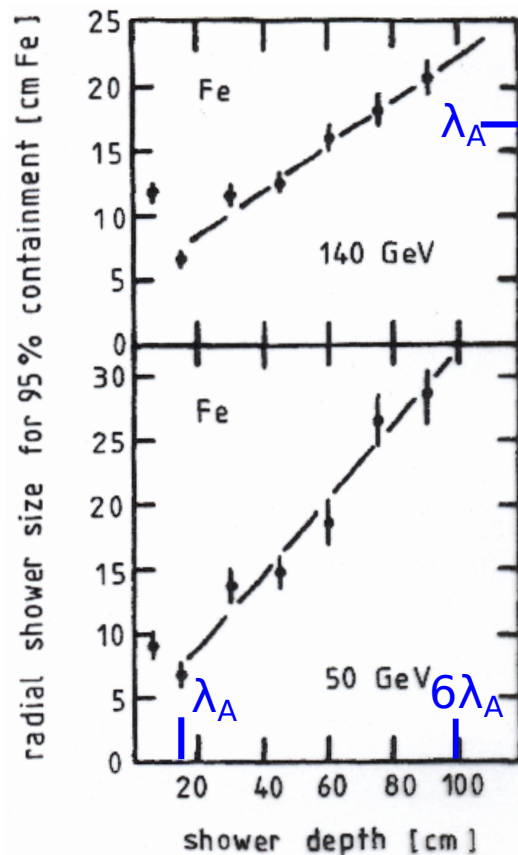
due to electromagnetic energy deposition rather sharp peak close to λ_A



π^+ in the CDHS Fe-scintillator calorimeter

Lateral shower development

- typical transverse momentum for secondary hadrons $\langle p_t \rangle \simeq 350 \text{ MeV}/c$
 lateral extent at shower maximum $R_{95} \simeq \lambda_A$
- relatively well defined core with $R \simeq R_M$ (electromagnetic component)
 - exponential decay (hadronic component and fluct. in interaction point)



9.2 Hadronic Calorimeters

homogeneous calorimeter that could measure entire visible energy loss generally too large and expensive

in any case fluctuations of invisible component make this expense unnecessary

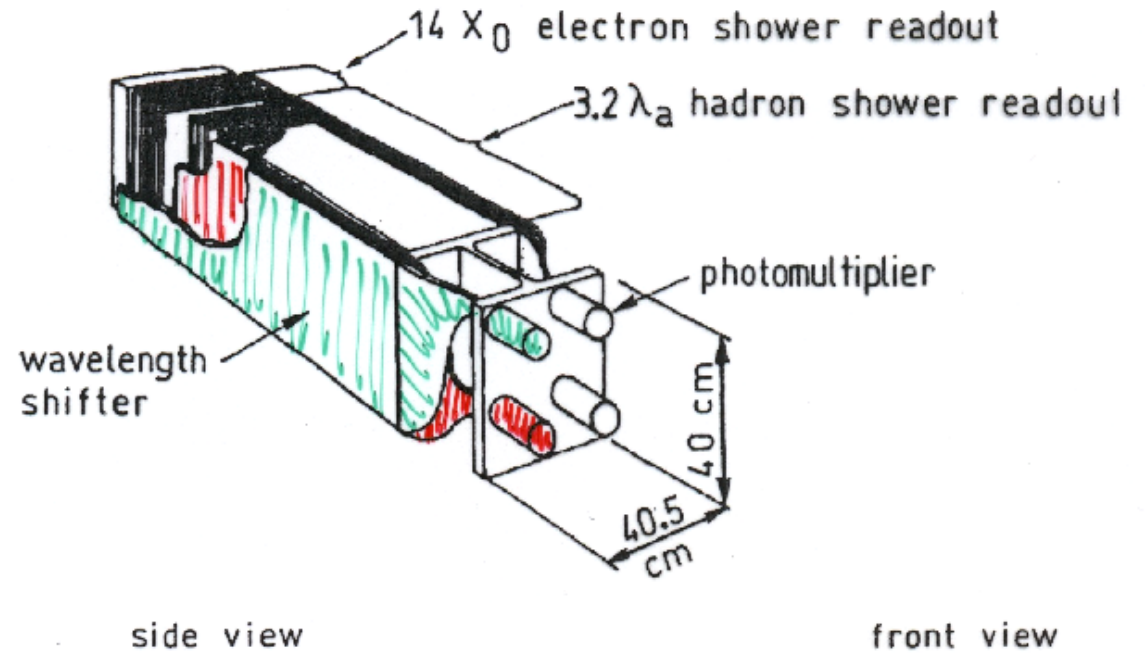
- most common realization: **sampling calorimeter**
passive absorber (Fe, Pb, U) + **sampling elements** (scintillator, liquid Ar or Xe, MWPC's, layers of proportional tubes, streamer tubes, Geiger-Müller tubes, ...)

typical setup

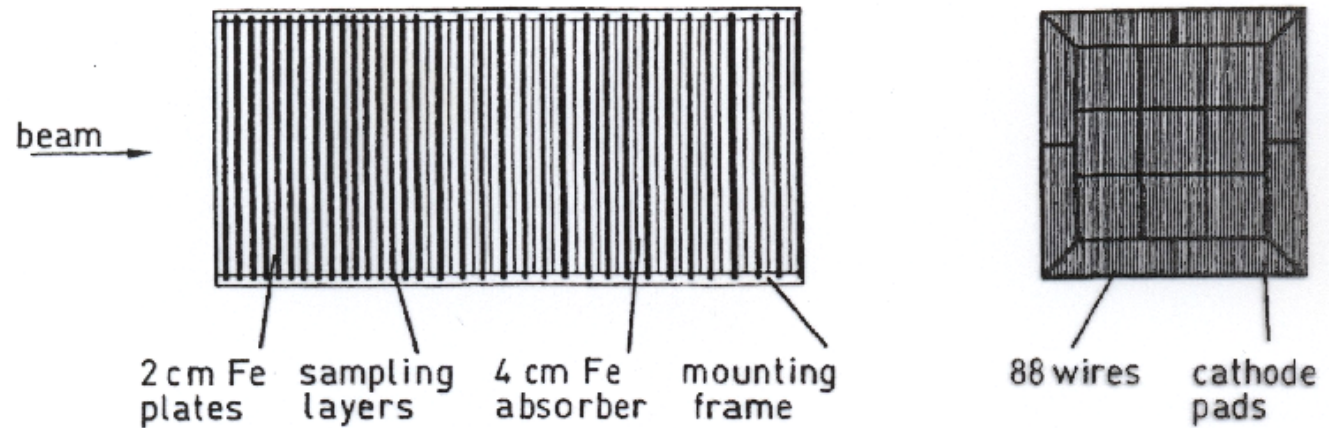
- alternating layers of active and passive material
- also spaghetti or shish kebab calorimeter (absorber with scintillating fibers embedded)

Typical arrangement of a sampling calorimeter

here: Fe/scint sampling calorimeter
 also: separation of electromagnetic and hadronic component possible



another example:
 Fe / streamer tube sampling calorimeter

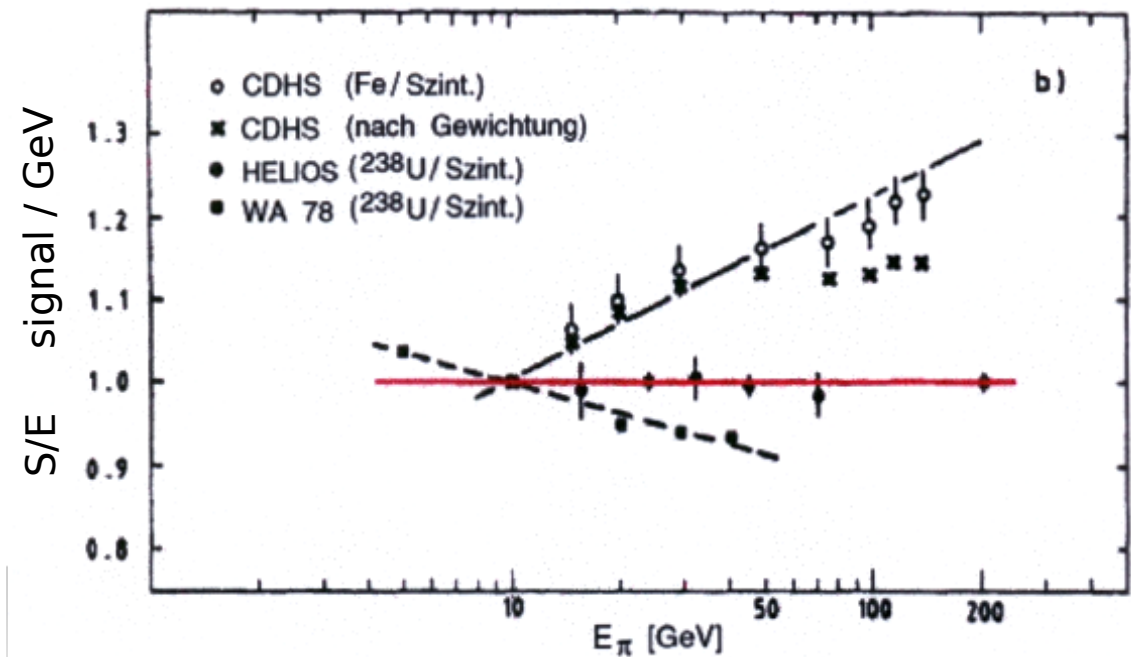


Quality of a calorimeter

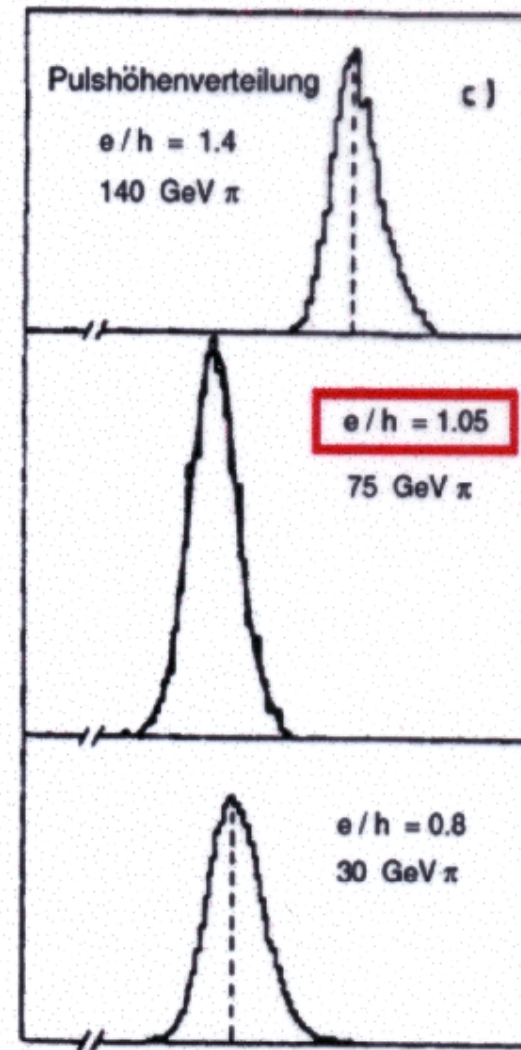
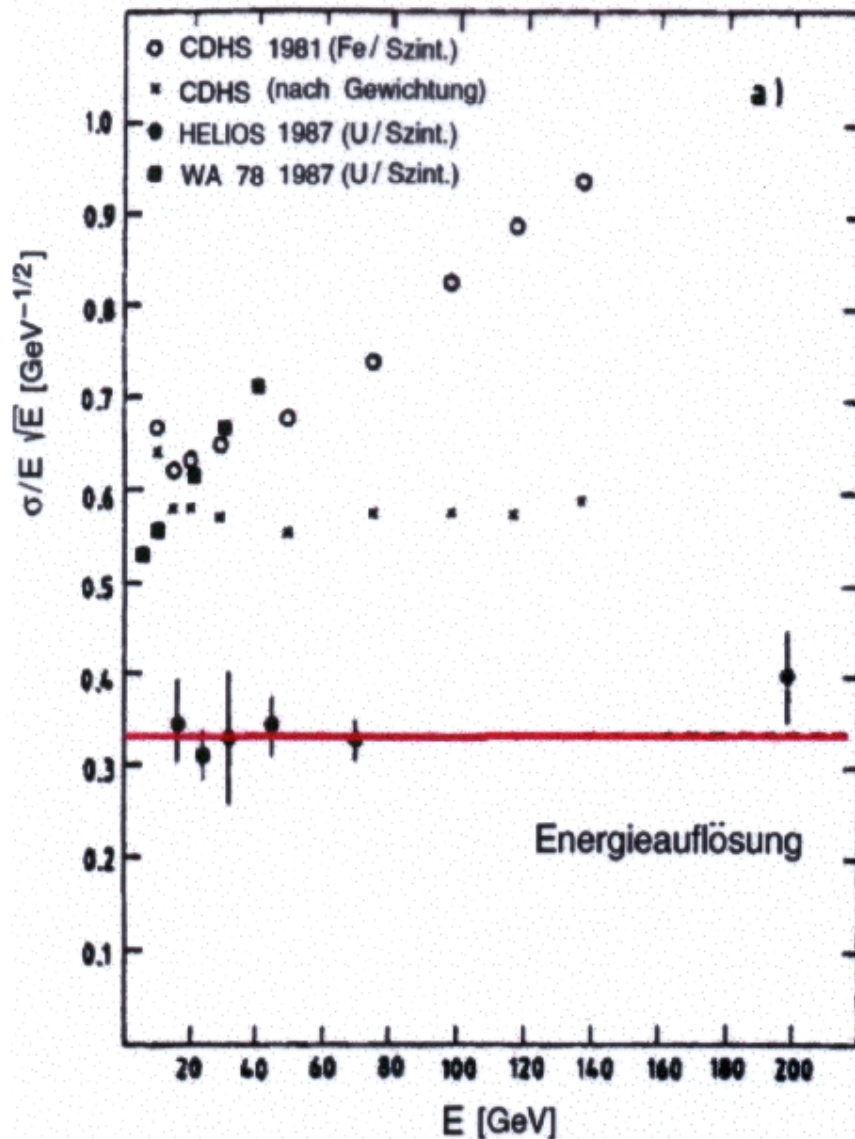
- linear response: $\text{signal} \propto E$
- energy resolution: $\frac{\sigma_E}{E} = \frac{\text{const}}{\sqrt{E}}$ fluctuations Poisson, respectively Gaussian
- signal independent of particle species

because of complicated structure of hadronic shower, typically not all 3 conditions completely met

i) response not completely linear



- ii) resolution deviates somewhat from $const/\sqrt{E}$
- iii) signal usually not completely Gaussian (tails), differences e vs h



where do these differences come from?

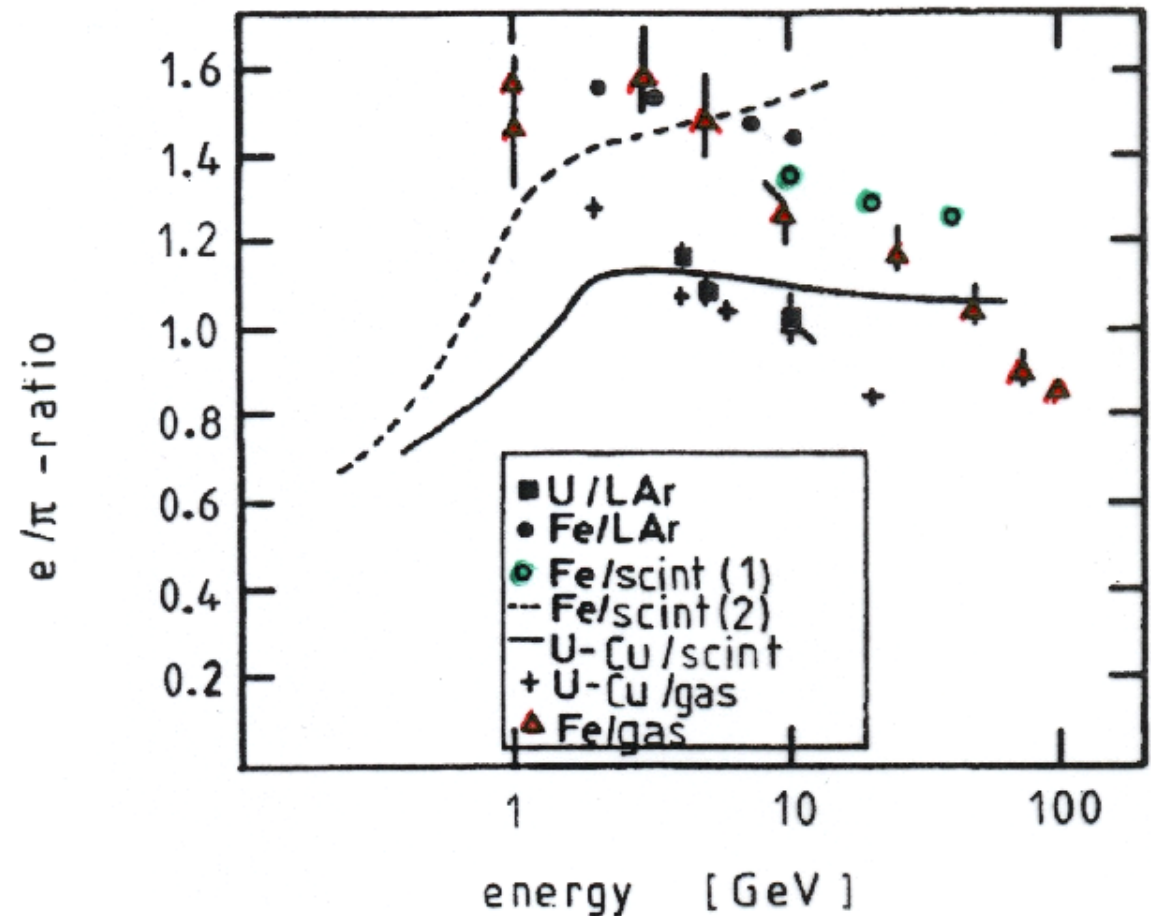
need to understand in order to optimize to come close to ideal

e/π big issue

generally response to electromagnetic and hadronic energy deposition different
usually higher weight to electromagnetic component, since hadronic shower has invisible component i.e. ' $e/h > 1$ '

why is this important? want to measure total energy flow in an event without resolving and identifying origin or composition of individual showers

different calorimeters do very differently!



optimization:

'compensation' (see below)

'overcompensation' if $e/\pi < 1$

Energy resolution

■ intrinsic contributions

- leakage and it's fluctuations

neutral and minimum ionizing particles:

neutrons with $\lambda \gg \lambda_A$,

muons,

neutrinos 'leakage fluctuations'

- fluctuations of electromagnetic portion

π^0 fluctuations combined with $e/h \neq 1$

- nuclear excitation, fission, spallation, binding energy fluctuations

- heavily ionizing particles with $dE/dx \gg (dE/dx)_{min.ion} \rightarrow$ saturation

all scale like $1/\sqrt{E}$ as statistical processes

■ sampling fluctuations

- dominate in electromagnetic calorimeter, nearly completely negligible in hadronic calorimeters: $\sigma_{sample}/S \propto \sqrt{d_{abs}/E}$ with d_{abs} = thickness of one absorber layer

■ other contributions

- noise: $\sigma_E/E = C/E$
- inhomogeneities: $\sigma_E/E = const$

contributions add in quadrature

$$\frac{\sigma_E}{E} = \frac{A}{\sqrt{E}} \oplus B \oplus \frac{C}{E}$$

A: 0.5 – 1.0 (record: 0.35)
B: 0.03 – 0.05
C: 0.01 – 0.02

typically dominated by leakage fluctuations

9.3 Compensation

how to get from $e/h > 1$ to $e/h \simeq 1$?

need understanding of contributions to signal \rightarrow allows optimization

particle i incident with energy $E(i)$

$$\text{visible energy} \quad E_v(i) = E_{dep}(i) - \underbrace{E_{nv}(i)}_{\text{invisible}}$$

$$\text{define visible fraction} \quad a(i) = \frac{E_v(i)}{E_v(i) + E_{nv}(i)}$$

compare various signals to those of a minimal ionizing particle:

$$\text{electron} \quad \frac{e}{mip} = \frac{a(e)}{a(mip)}$$

$$\text{hadronic shower component} \quad \frac{h_i}{mip} = \frac{a(h_i)}{a(mip)}$$

$$\text{electron signal} \quad S(e) = k \cdot E \cdot \frac{e}{mip}$$

$$\text{hadronic signal} \quad S(h_i) = k \cdot E \cdot \left[f_{em} \frac{e}{mip} + (1 - f_{em}) \frac{h_i}{mip} \right]$$

constant k determined by calibration

f_{em} : fraction of primary energy of a hadron deposited in form of electromagnetic energy
 $\approx \ln(E/1 \text{ GeV})$

$$\text{in case } \frac{e}{mip} \neq \frac{h_i}{mip} \rightarrow \frac{S(h_i)}{E} \neq \text{const.}$$

$$\frac{S(e)}{S(h_i)} = \frac{e/mip}{f_{em}(e/mip) + (1 - f_{em})(h_i/mip)}$$

→ worsening of resolution in case $e/mip \neq h_i/mip$

→ $S/E \neq \text{constant}$

$$\text{aim for } \frac{e}{mip} = \frac{h_i}{mip} \rightarrow \frac{S(e)}{S(h_i)} = 1$$

hadronic shower has various contributions to its visible energy

$$\frac{h_i}{mip} = f_{ion} \frac{ion}{mip} + f_n \frac{n}{mip} + f_\gamma \frac{\gamma}{mip} + f_b \frac{b}{mip}$$

f_{ion} fraction of hadronic component in charged particles, ionizing (μ^\pm, π^\pm, p)

f_n fraction of neutrons

f_γ fraction of photons

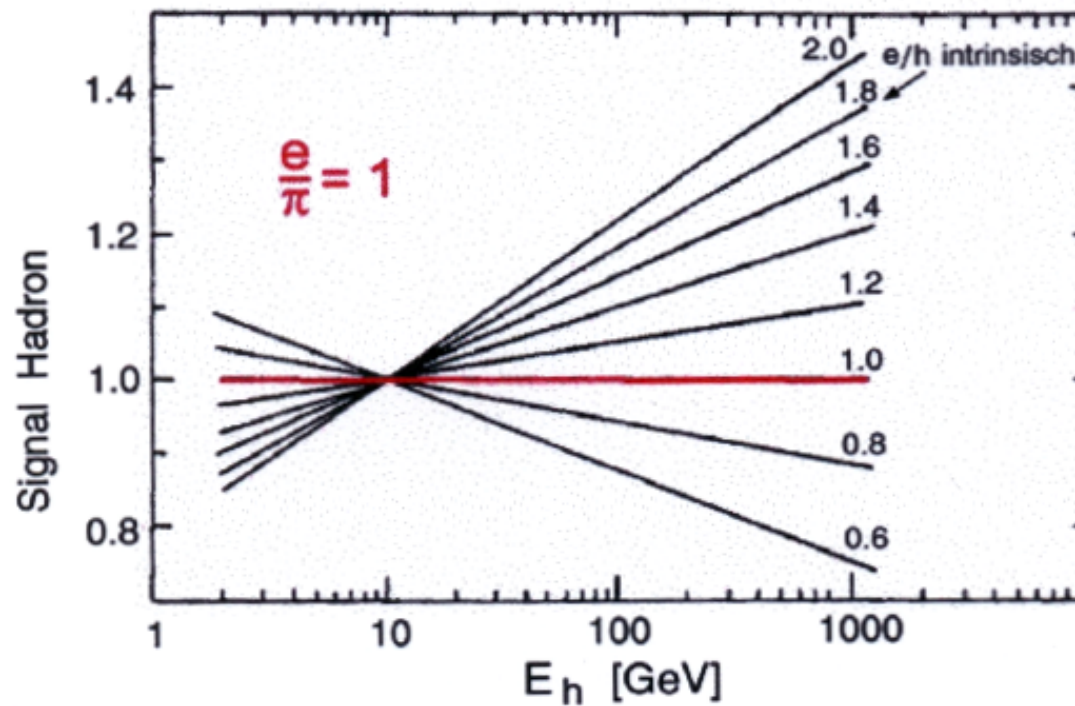
f_b fraction of nuclear binding energy

example: 5 GeV proton

	Fe	U	
f_{ion}	57%	38%	← dominated by spallation products (protons)
f_γ	3%	2%	
f_n	8%	15%	} strongly correlated
f_b	32%	45%	

	Fe/Sci	Fe/Ar	U/Sci	U/Ar	determined by
ion/mip	0.83	0.88	0.93	1.0	d_{act}
n/mip	0.5-2	0	0.8 - 2.5	0	d_{act}/d_{abs}
γ/mip	0.7	0.95	0.4	0.4	d_{abs}
e/mip	0.9	0.95	0.55	0.55	d_{abs}

increase h_i/mip via increase of f_n , f_γ (materials) and n/mip , γ/mip (layer thicknesses)

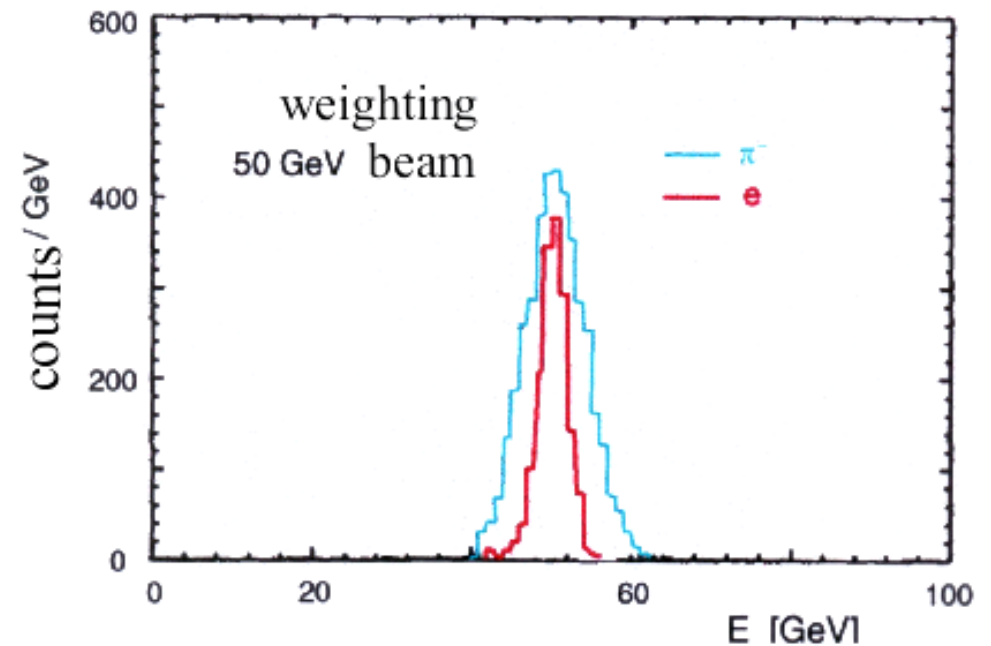
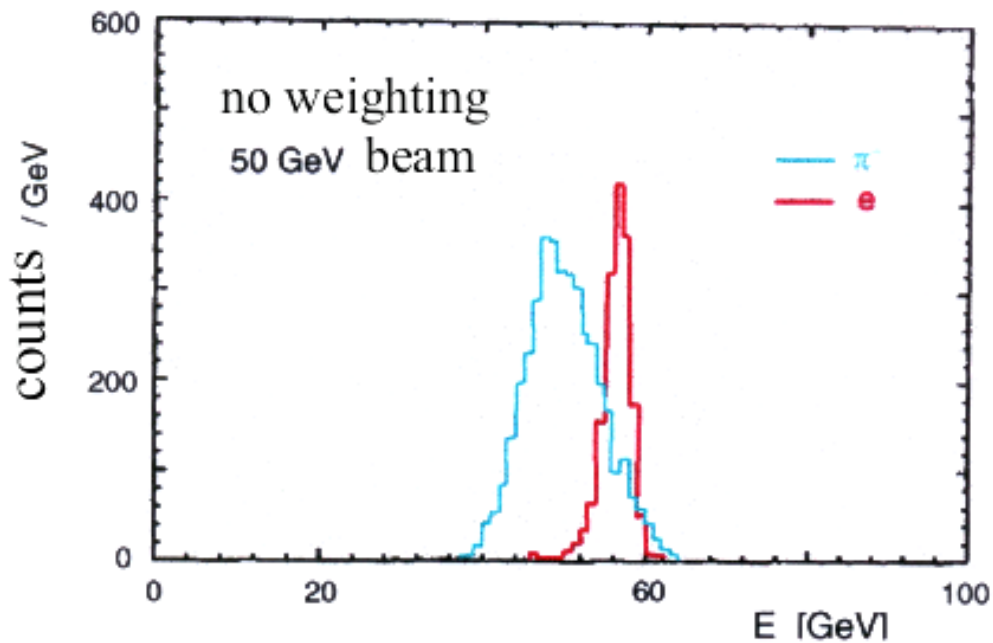


hadron signal in different sampling calorimeters

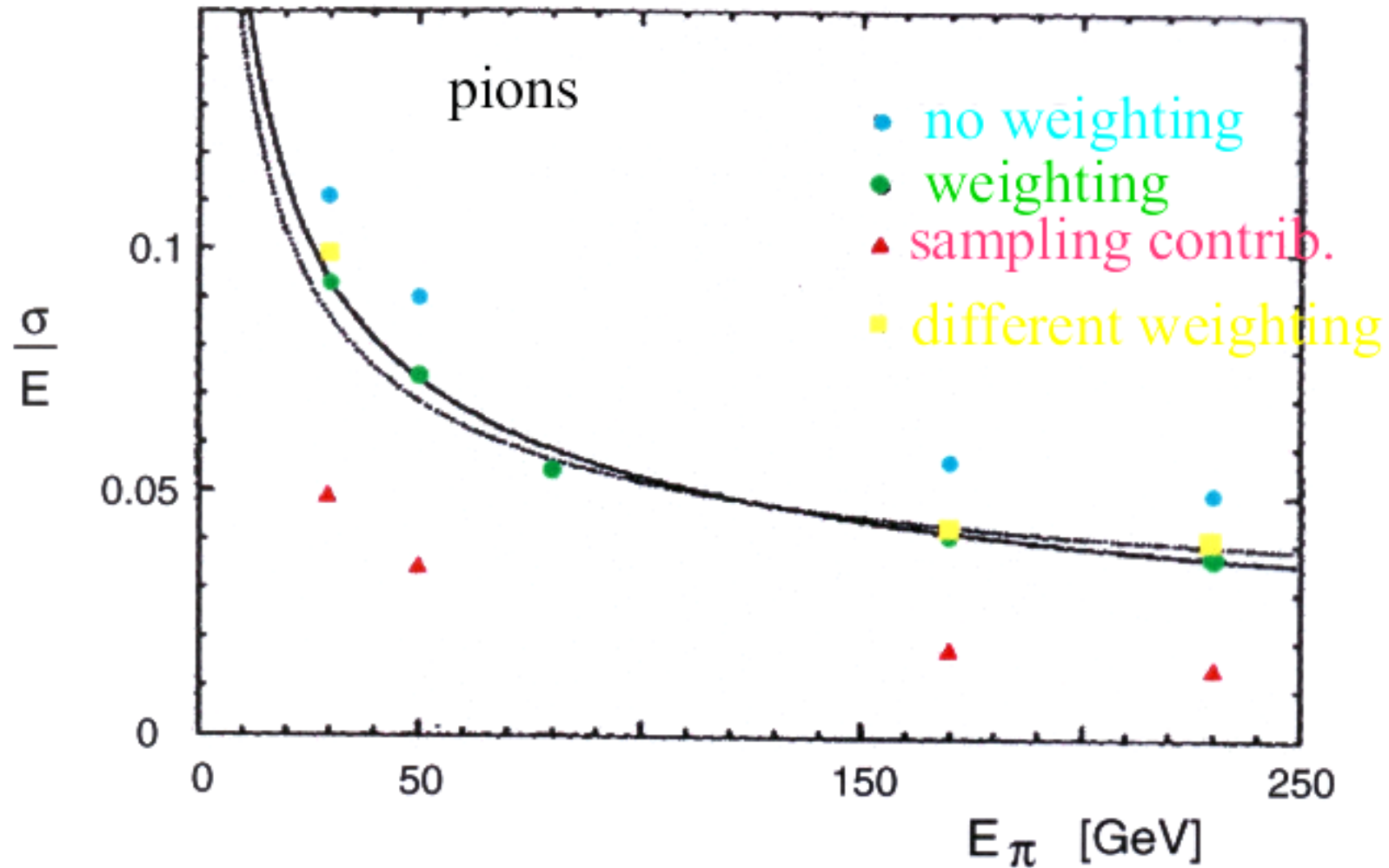
Software compensation

- segmentation in depth layers
- identify layers with particularly large $E_v \rightarrow \pi^0$ contribution
- small weight for these layers

$$w_i^* = w_i(1 - cw_i) \quad w_i : \text{measured, deposited energy} \quad c : \text{weight factor}$$



Energy resolution of non-compensating liquid-Ar calorimeter



with weighting overall response more Gaussian, improved resolution, improved linearity

Hardware compensation

essential, if one wants to trigger!

increase of h/mip or decrease of e/mip

- increase of hadronic response via fission and spallation of ^{238}U

$$\uparrow \frac{ion}{mip} \text{ or } \frac{n}{mip}$$

- increase of neutron detection efficiency in active material \rightarrow high proton content

$$Z = 1 \rightarrow \uparrow \frac{n}{mip}$$

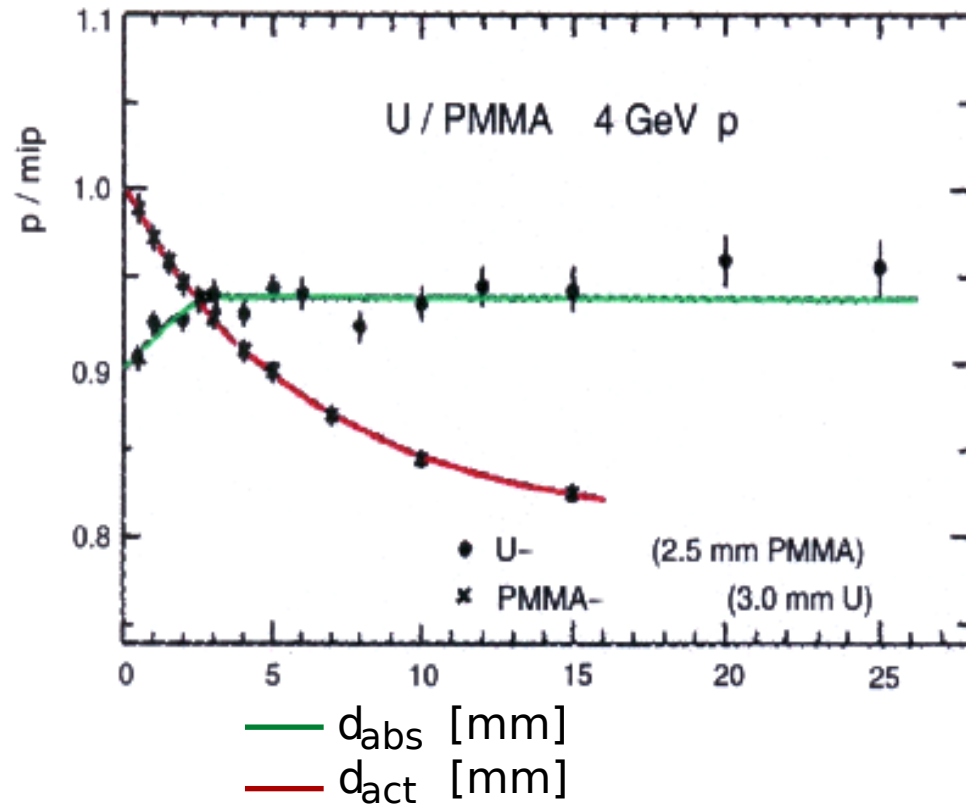
- reduction of e/mip via high Z absorber and suitable choice of $\frac{d_{abs}}{d_{act}}$

$$Z_{abs} \uparrow \rightarrow \downarrow \frac{e}{mip} \leftarrow \uparrow d_{abs}$$

- long integration time \rightarrow sensitivity to γ capture after neutron thermalization

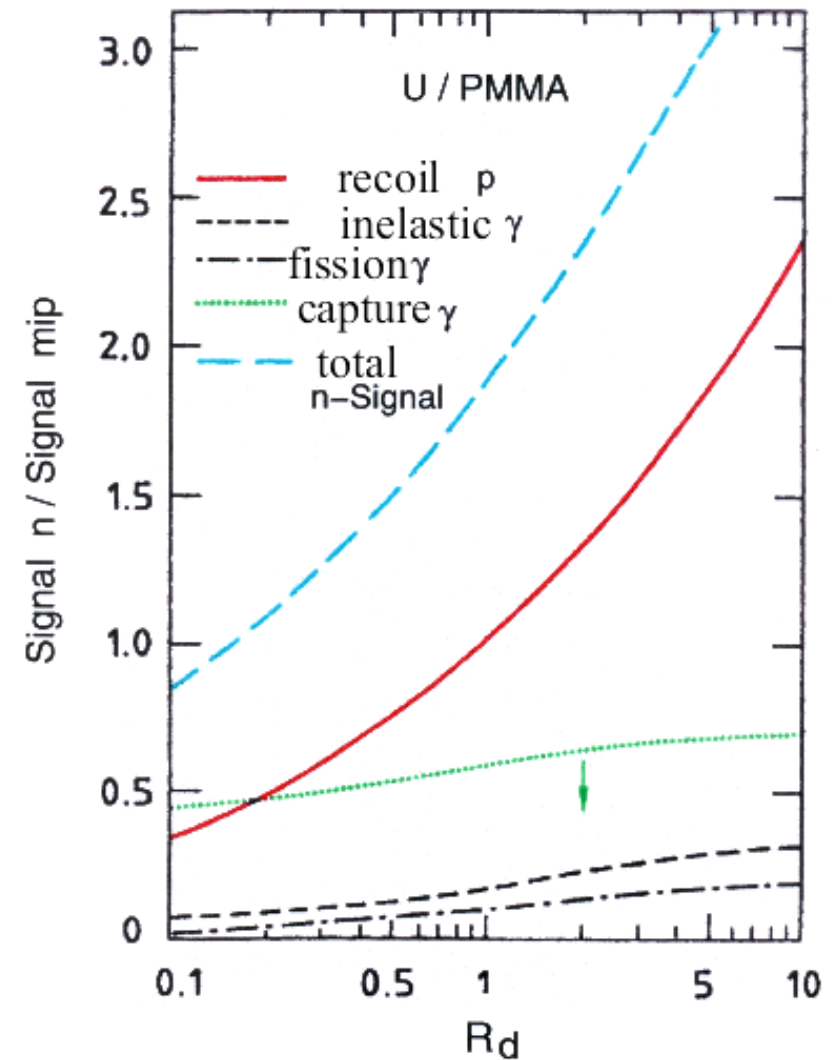
$$t \text{ long} \rightarrow \uparrow \frac{n}{mip}$$

calorimeter response to protons



variation of plate thickness \leftrightarrow variation of response p/mip

calorimeter response to neutrons



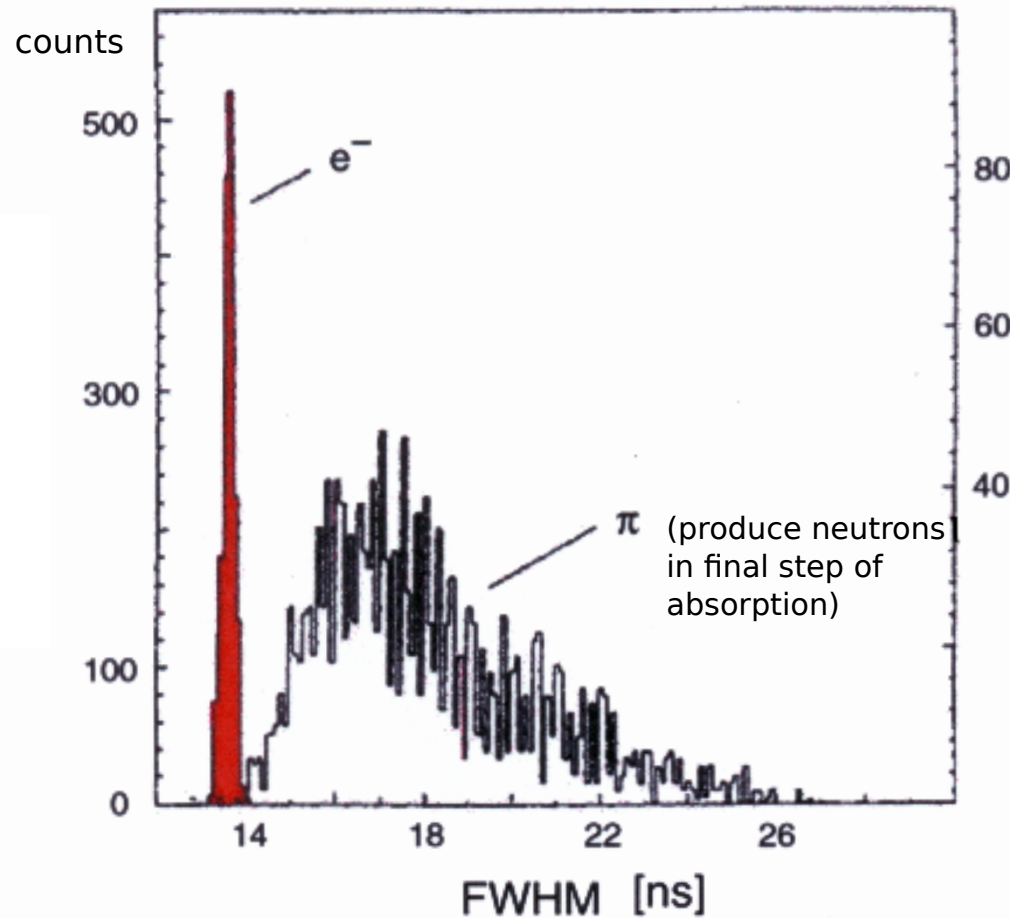
variation of contributions vs. $R_d = d_{abs}/d_{act}$

time structure different for electron and hadron showers

in em shower, all components cross detector within few ns (speed basically 30 cm/ns)

in hadronic shower component due to neutrons is delayed, need to slow down before they produce visible signal

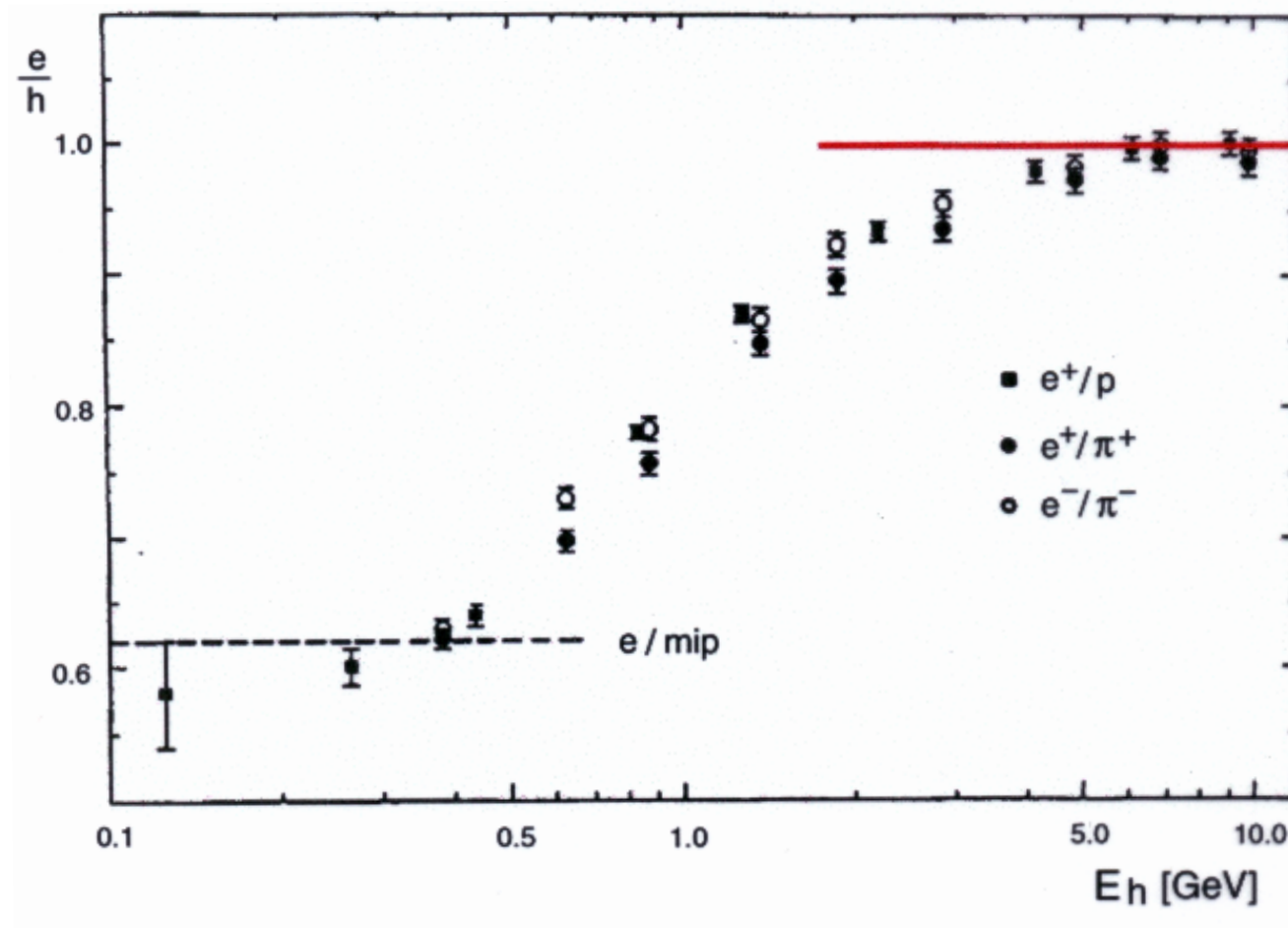
signal width for 80 GeV e^- and π in spaghetti calorimeter



size of signal depends on integration time – variation in integration time of electronics can enhance hadronic signal (used in ZEUS calorimeter)

the e/π problem of hadronic calorimeters

U (3 mm) + Scintillator (2.5 mm)



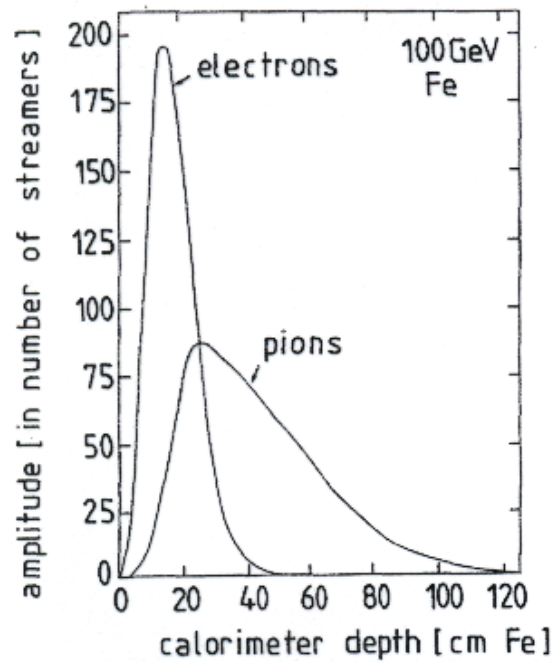
measured ratio of electron/pion signals at (ZEUS) for $E \geq 3$ GeV nearly compensated

9.4 Particle identification

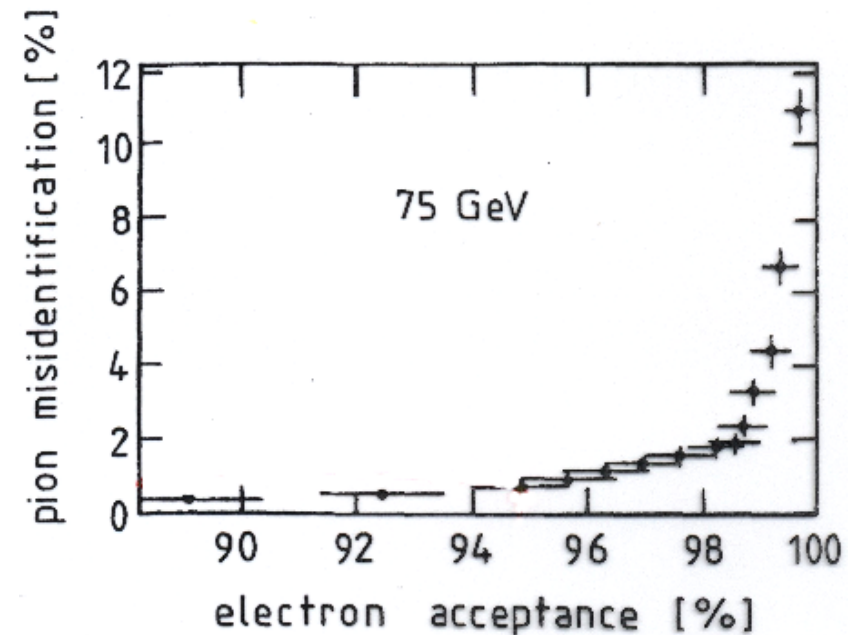
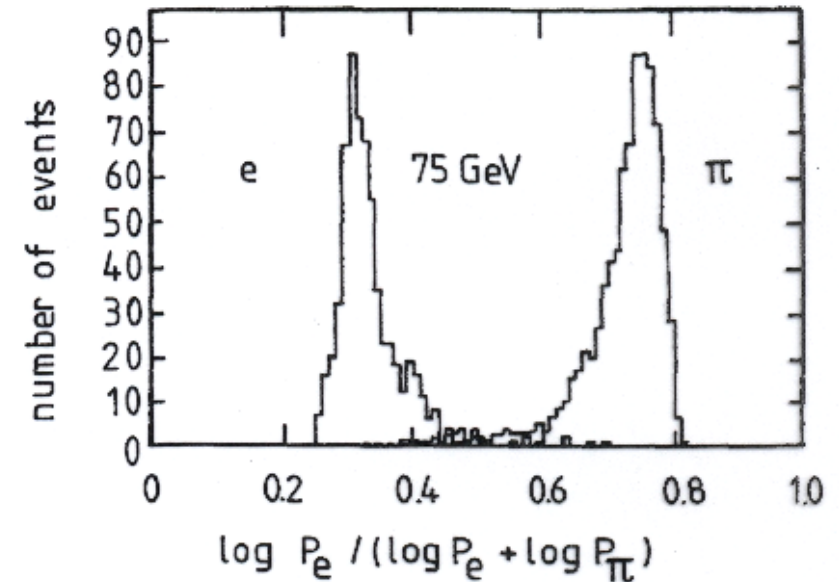
electron/pion:

- use difference in transverse and longitudinal shower extent
- signal for electron is faster

hadron showers are deeper and wider and start later
PID based on likelihood analysis

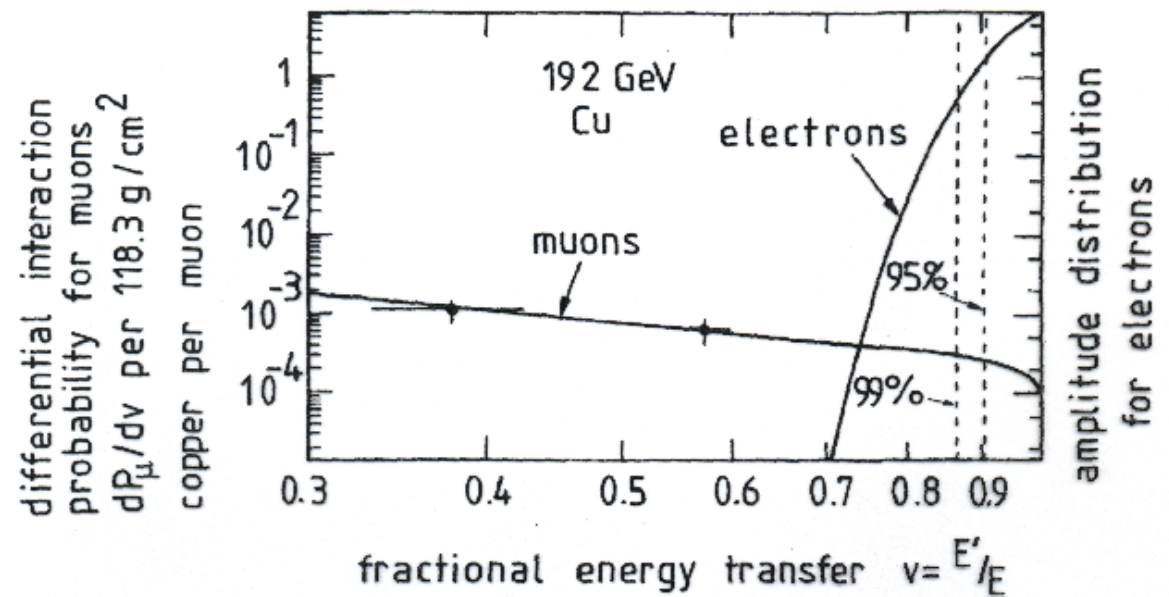
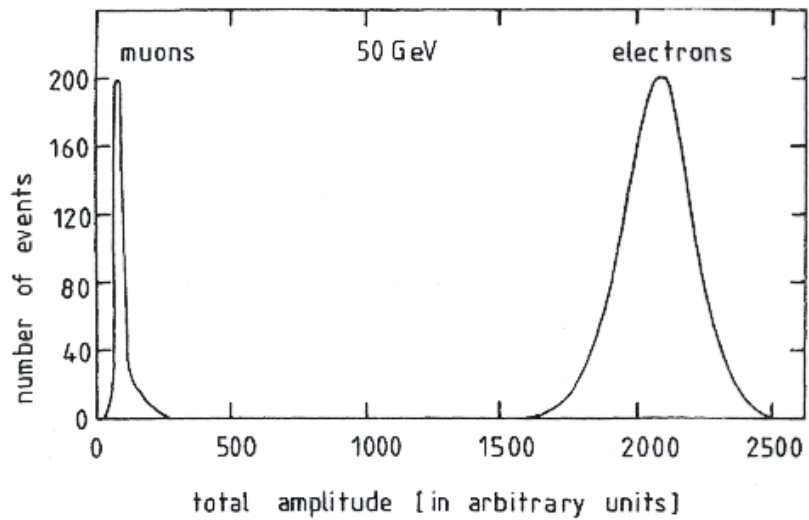


streamer tube calorimeter



Muon vs pion/electron

low energy loss for muon



for 95% electron efficiency muon probability $1.7 \cdot 10^{-5}$

9.5 Role of (hadronic) calorimeters in large experiments

increasing importance compared to momentum measurement as energy increases

$$\frac{\sigma_p}{p} = A \oplus B \cdot p \quad \text{good: } B = 0.1\%$$

$$\frac{\sigma_E}{E} = \frac{A}{\sqrt{E}} \oplus B \oplus \frac{C}{E}$$

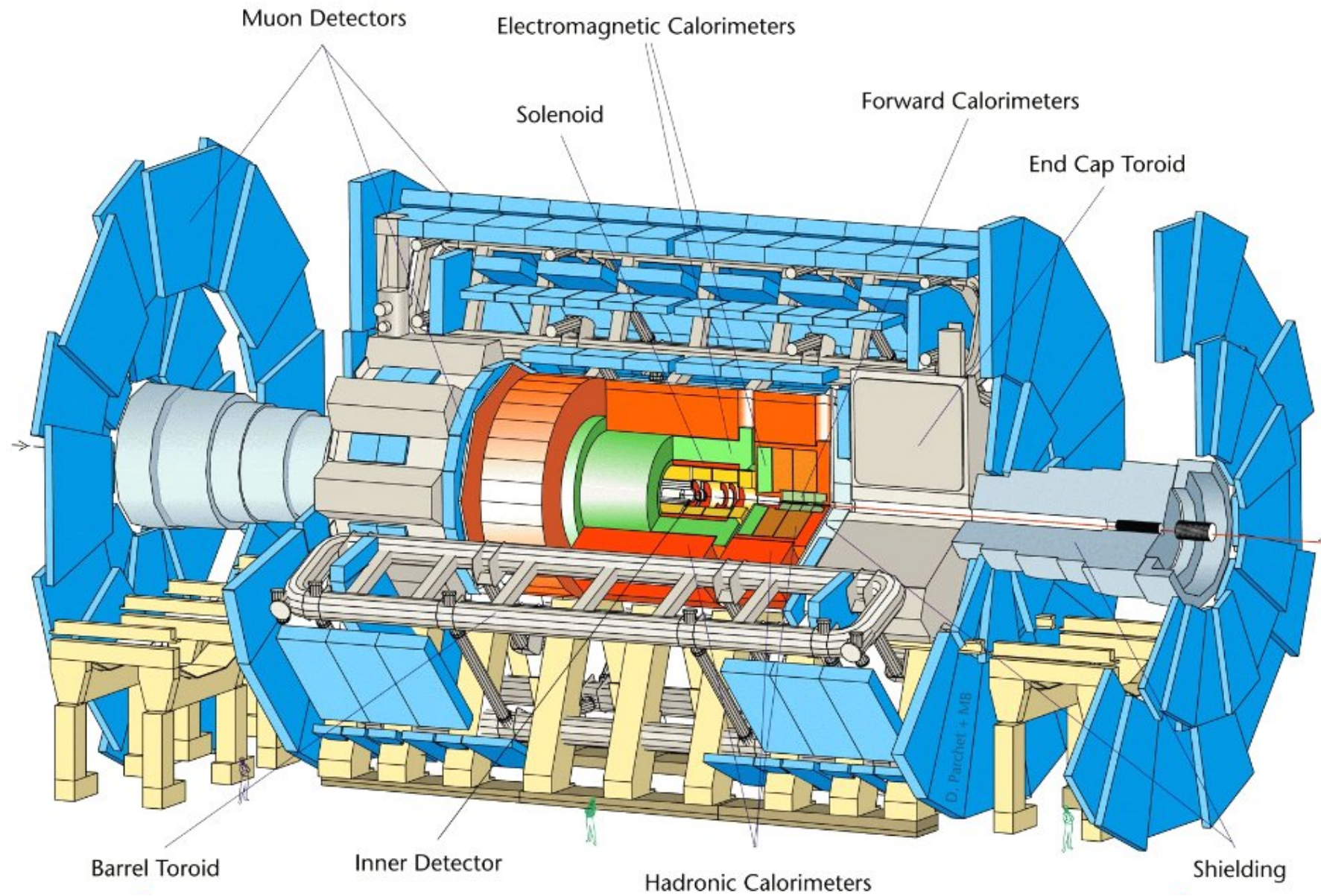
ATLAS hadronic calorimeter $A \simeq 0.50$, $B \simeq 0.033$, $C = 0.018$

hadronic shower in ATLAS

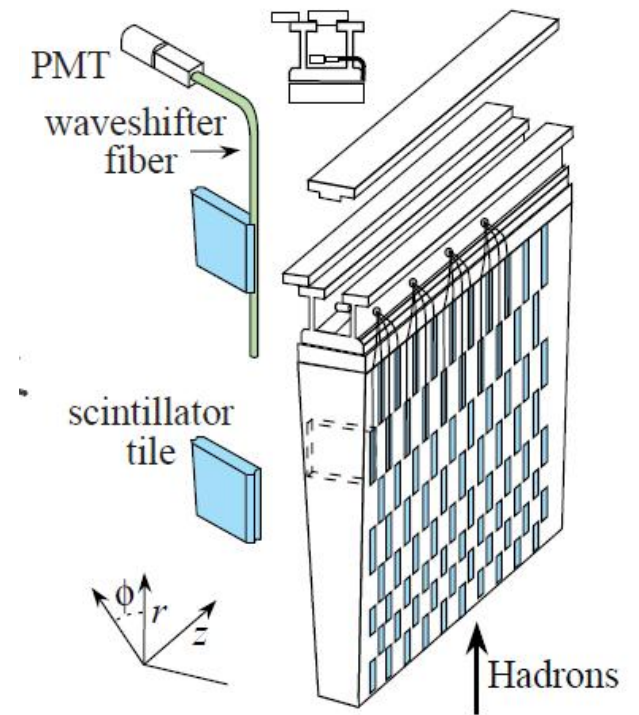
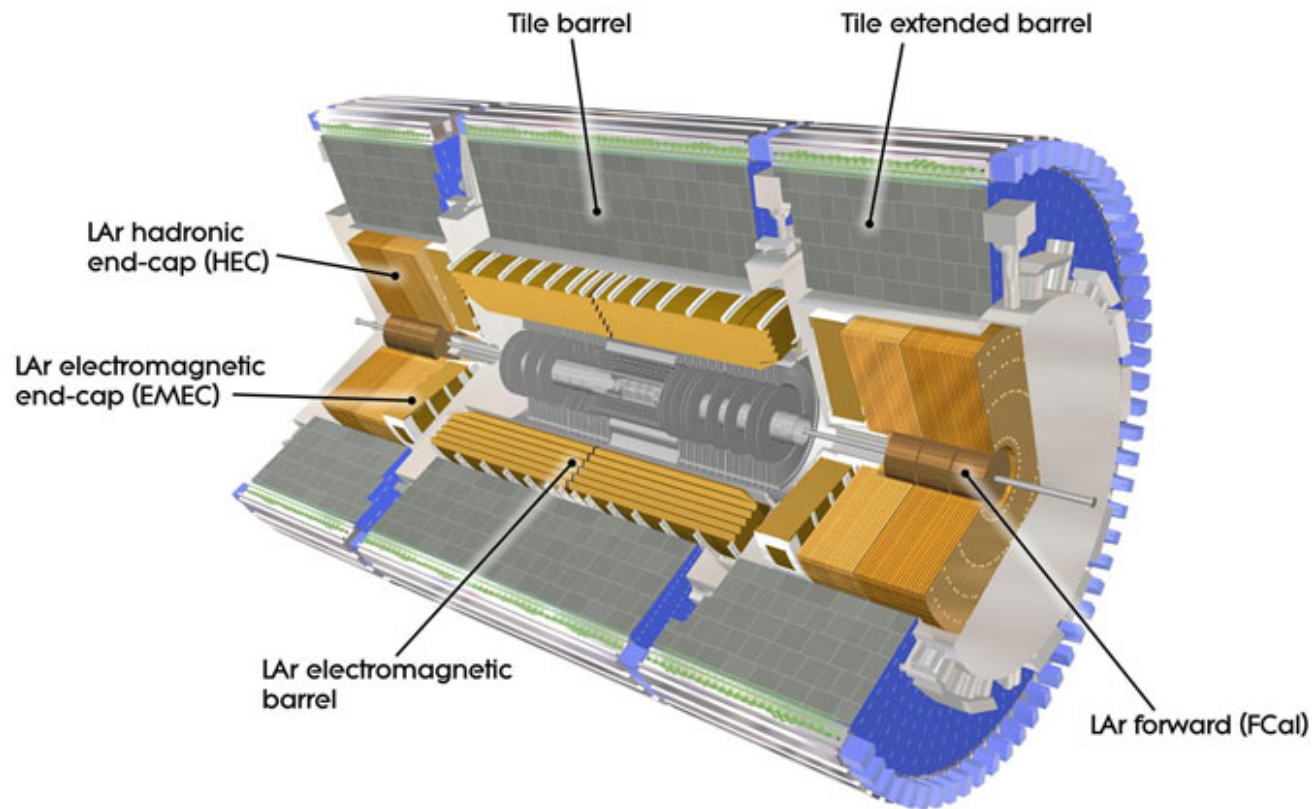
- visible EM \sim (50%)
 - e , γ , π^0
- visible non-EM \sim (25%)
 - ionization of π , p , μ
- invisible \sim (25%)
 - nuclear break-up
 - nuclear excitation
- escaped \sim (2%)

$$E = 1000 \text{ GeV} \quad \rightarrow \quad \frac{\sigma_E}{E} = 0.04$$

$$\frac{\sigma_p}{p} = 1.00$$



overall layout of the ATLAS detector

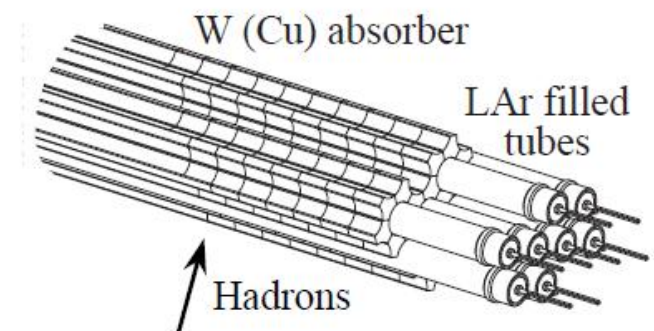


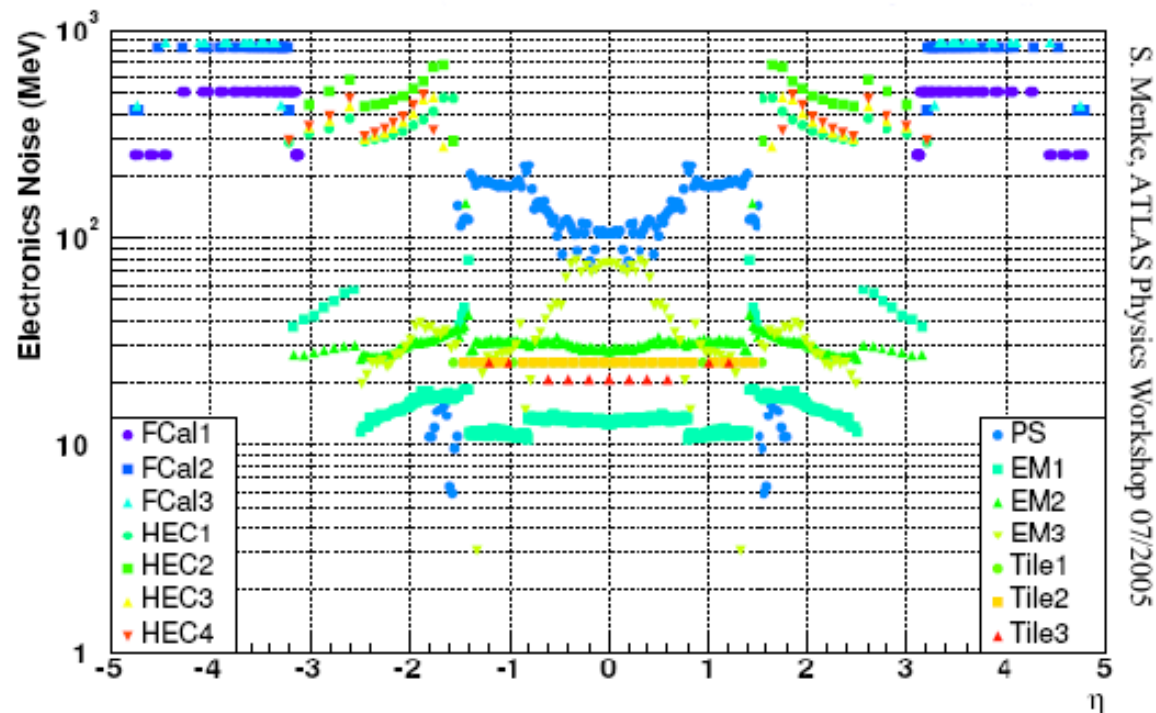
hadronic tile calorimeters:

steel sheets and scintillator tiles read out with wavelength-shifting fibers radially along outside faces into PMTs

forward hadronic calorimeters:

tubes with LAr embedded into tungsten matrix



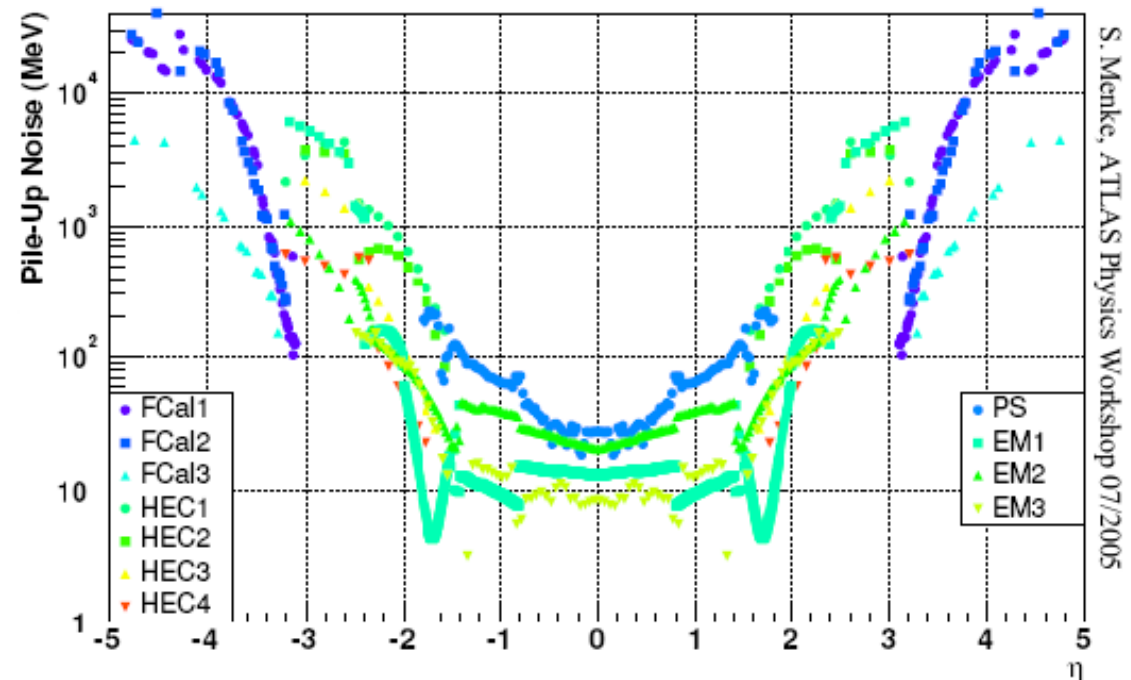


S. Menke, ATLAS Physics Workshop 07/2005

electronic noise in calorimeter cells
10 MeV – 850 MeV

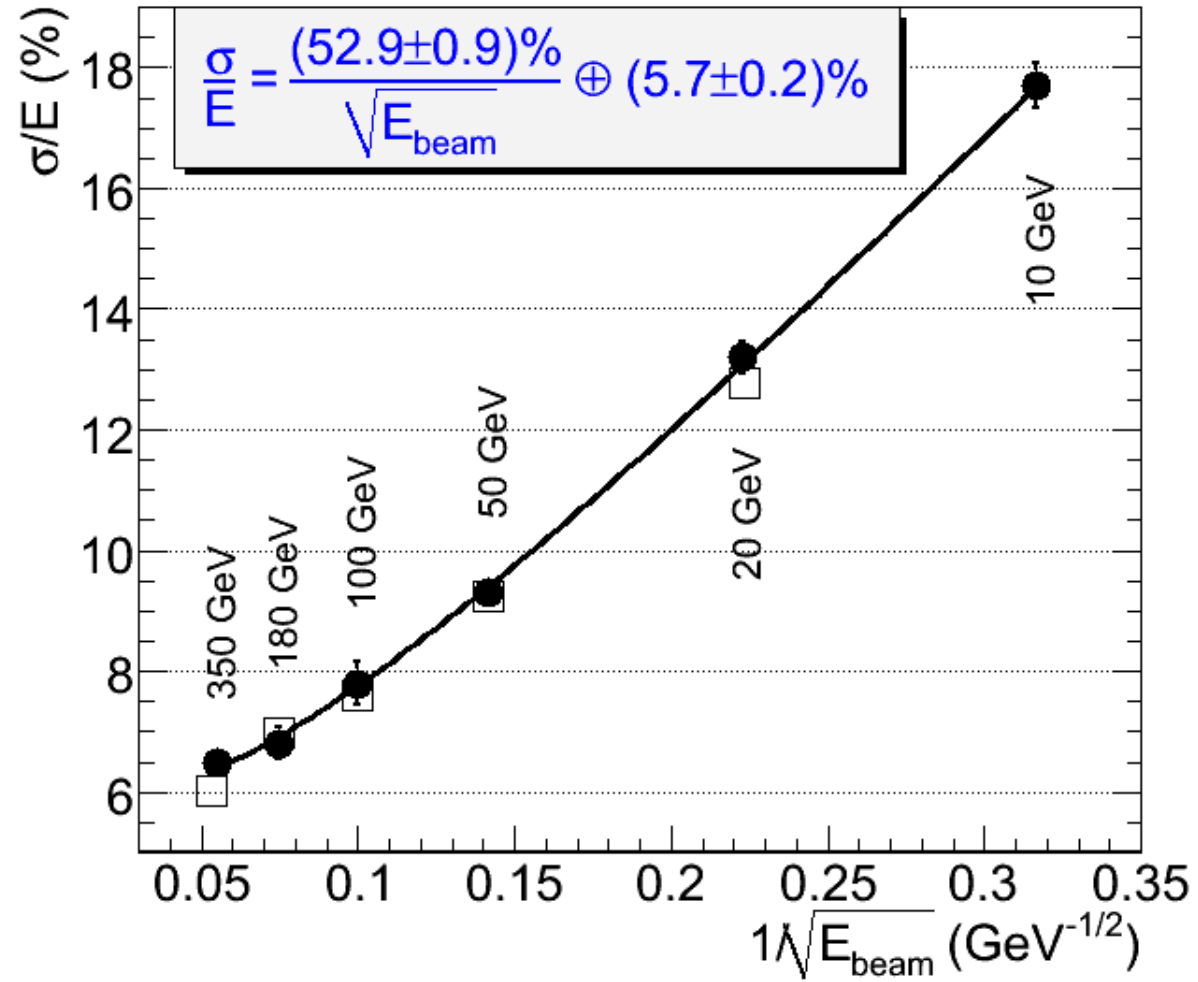
pile-up noise in calorimeter cells

many events piling up on top of each other
introduces asymmetric cell signal fluctuations
from ~ 10 MeV (rms, central region)
up to ~ 40 MeV (rms, forward)
similar to coherent noise

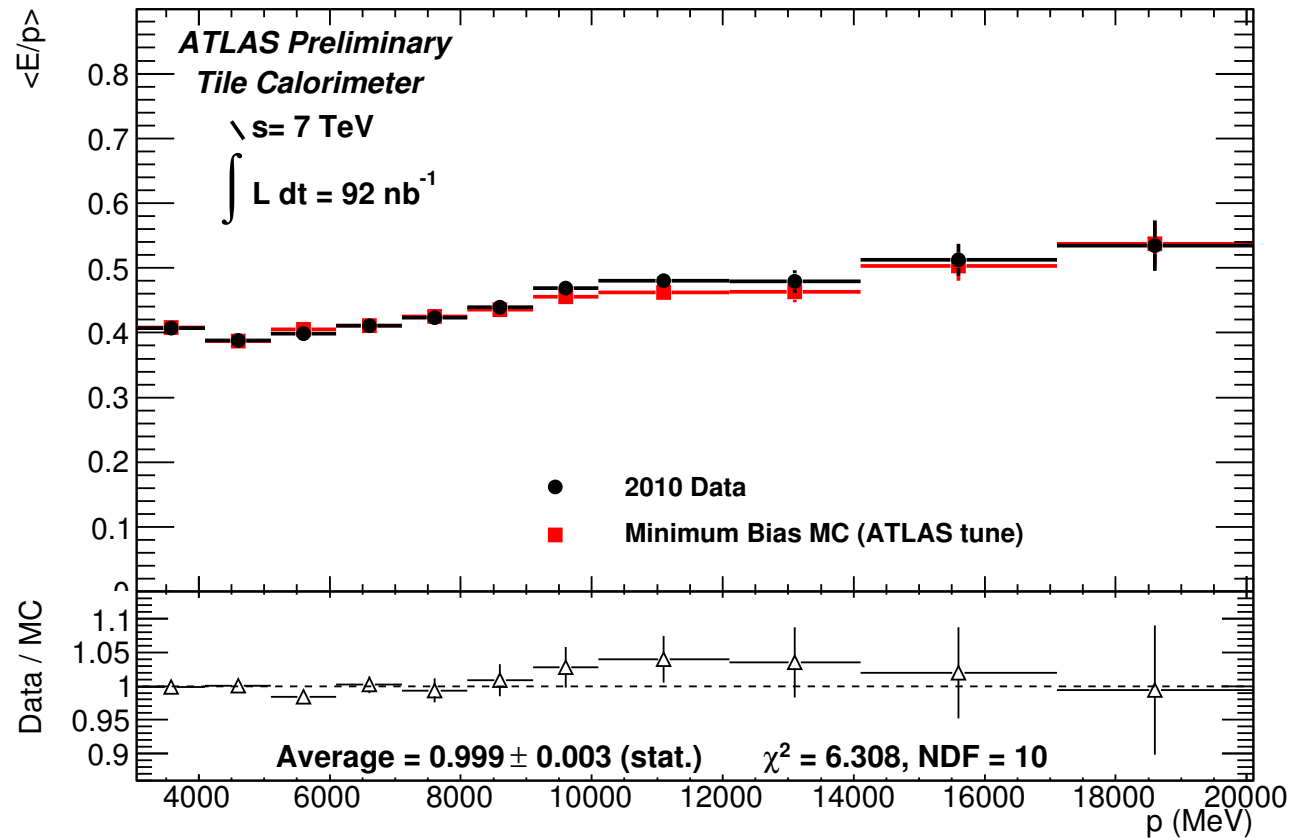


S. Menke, ATLAS Physics Workshop 07/2005

ATLAS tile calorimeter pion energy resolution



ATLAS tile calorimeter response to hadrons



response for isolated tracks that look like mips in EMCal